Journal of Earth Science, *Vol. 27*, *No. 5*, *p. 796–806*, *October 2016* *ISSN 1674-487X*
Printed in China
DOI: 10.1007/s12583-016-0909-8

Paleogeothermal Reconstruction and Thermal Evolution Modeling of Source Rocks in the Puguang Gas Field, Northeastern Sichuan Basin

Chuanqing Zhu*[1, 2], Nansheng Qiu[1, 2], Huanyu Cao[3], Song Rao[4], Shengbiao Hu[5]
1. *State Key Laboratory of Petroleum Resources and Prospecting*, *China University of Petroleum*, *Beijing* 102249, *China*
2. *College of Geosciences*, *China University of Petroleum*, *Beijing* 102249, *China*
3. *Exploration Branch*, *SINOPEC*, *Chengdu* 610041, *China*
4. *College of Geosciences*, *Yangtze University*, *Jingzhou* 434023, *China*
5. *State Kay Laboratory of Lithospheric Evolution*, *Institute of Geology and Geophysics*, *Chinese Academy of Sciences*, *Beijing* 100029, *China*

ABSTRACT: The thermal history and organic matter maturity evolution of the source rocks of boreholes in the Puguang gas field were reconstructed. An integrated approach based on vitrinite reflectance and apatite fission track data was used in the reconstruction. Accordingly, the geothermal conditions of gas accumulation were discussed in terms of the geological features of reservoirs in the northeastern Sichuan Basin. The strata reached their maximum burial depth in the Late Cretaceous era and were then uplifted and denuded continuously to the present day. The geothermal gradient and heat flow in the Late Cretaceous era were approximately 30.0 °C/km and 66 mW/m^2, respectively, which were both higher than those at present. The tectonothermal evolution from the Late Cretaceous era to the present is characterized by denudation and cooling processes with an erosion thickness of ~2.7 km. In addition to the Triassic era, the Jurassic era represents an important hydrocarbon generation period for both Silurian and Permian source rocks, and the organic matter maturity of these source rocks entered into a dry gas period after oil generation. The thermal conditions are advantageous to the accumulation of conventional and unconventional gas because the hydrocarbon generation process of the source rocks occurs after the formation of an effective reservoir cap. In particular, the high geothermal gradient and increasing temperature before the denudation in the Late Cretaceous era facilitated the generation of hydrocarbons, and the subsequent cooling process favored its storage.

KEY WORDS: paleogeothermal reconstruction, apatite fission track, vitrinite reflectance, thermal evolution of source rocks, Puguang gas field.

0 INTRODUCTION

The thermal states of sedimentary basins affect hydrocarbon generation, migration, and accumulation processes, and therefore reconstructing a basin's thermal history is significant for petroleum accumulation analyses. The maturity of organic matter is primarily controlled by the temperature of the source rock (Tissot and Pelect, 1987; Tissot and Welte, 1984). Given the geothermal dependence of hydrocarbon generation, several researchers consider the geothermal gradient (geotherm) to be another significant controlling factor for oil and gas accumulation, in addition to its role in the evolution of oil and gas in source rocks. According to the "co-control by source and heat" theory of Zhang (2012), the type of thermal field determines the intensity of heating in a basin and its source rocks. Different thermal evolution histories of hydrocarbon source rocks are controlled by the thermal setting of the basin and their burial histories (Zhang, 2014, 2012).

Northeastern Sichuan produces a large amount of natural gas from basins in various regions, including the Puguang and Yuanba gas fields. The thermal history of these regions has been investigated following their exploration and exploitation. However, existing studies have mainly reconstructed the thermal history of these regions using single methods such as vitrinite reflectance or thermophysical property data to simulate the thermal history and/or hydrocarbon source rock history. The results indicated that the paleo-heat flow reached its maximum values of 62 to 70 mW/m^2 around 255 Ma, then began to decrease until the present. The greatest denudation of the basins is marked by the Mesozoic–Cenozoic unconformity and reached a maximum of approximately 2 100 m (Lu et al., 2005). Apatite fission track (AFT) and (U-Th)/He radiometric dating methods

*Corresponding author: zhucq@cup.edu.cn
© China University of Geosciences and Springer-Verlag Berlin Heidelberg 2016

Manuscript received March 16, 2015.
Manuscript accepted March 14, 2016.

Zhu, C. Q., Qiu, N. S., Cao, H. Y., et al., 2016. Paleogeothermal Reconstruction and Thermal Evolution Modeling of the Source Rocks in the Puguang Gas Field, Northeastern Sichuan Basin. *Journal of Earth Science*, 27(5): 796–806. doi:10.1007/s12583-016-0909-8. http://en.earth-science.net

have been used to study uplift and denudation history (Tian et al., 2012, 2011; Mei et al., 2010; Shen et al., 2007) and suggest three possible cooling histories, namely: linear cooling since 100 Ma, slow cooling since 100 Ma followed by enhanced cooling since 40 Ma, and slow cooling since 100 Ma followed by enhanced cooling since 30 Ma. The total post-Early Cretaceous denudation of the northeastern Sichuan Basin is estimated at 5 km (Tian et al., 2011). Only thermal history has been emphasized in the literature although geothermal thermochronometry and vitrinite reflectance data were simultaneously considered in analyzing thermal history or thermal evolution of source rocks (Qiu et al., 2008), and maturity has also been forward modeled using estimated parameters (Wu and Peng, 2013; Rao et al., 2011). Consequently, the denudation process (erosion thickness and periods) and the paleogeothermal gradient before denudation, which are dominant factors in the thermal evolution of source rocks, have not been discussed in detail. This study combines vitrinite reflectance and AFT data to reconstruct the thermal history and evolution of source rocks in boreholes in the Puguang gas field. Geological features of oil and gas accumulation are discussed as well as the geothermal conditions of natural gas accumulation.

1 GEOLOGICAL BACKGROUND

The northeastern Sichuan area is located to the south of the Micang Mountain bulge in front of the Micang-Daba Mountain arcuate tectonic zone in the northeastern part of the Sichuan Basin (Fig. 1). The eastern Sichuan foreland fold-thrust belt is the main structure in this region (Zheng et al., 2008). Marine carbonates were primarily deposited during the Neopaleozoic era, and thick foreland basin sediments were deposited during the Mesozoic era. Devonian–Lower Carboniferous strata rarely formed in this region as a consequence of Caledonian earth movements, and Middle Jurassic strata were subsequently uplifted to the surface.

The strata in northeastern Sichuan include many combinations of potential reservoir rocks which provide advantageous conditions for hydrocarbon accumulation. Four sets of marine source rocks were developed, including the Lower Cambrian Niutitang Formation, Upper Ordovician Wufeng–Lower Silurian Longmaxi Formation, Lower Permian Formation, and Upper Permian Formation (Tenger et al., 2012; 2010; Liang et al., 2008; Huang et al., 1996). The hydrocarbon of the Puguang gas field mainly originates from Permian and Silurian (mostly Permian) source rocks (Tenger et al. 2012; Ma, 2010; Ma et al., 2007a; Cai et al., 2005).

The reservoir strata of the Puguang gas field are mainly combinations of flat reef dolomites at the margin of the Permian Changxing Formation (P*ch*) platform and grain shoal oolitic deposits representing beaches of shallow to open sea platform facies in the Triassic Feixianguan Formation (T_1f). Gypsum salt rocks were developed during the Mid-Triassic era in sections 2 and 4 of the Lower Triassic Jialingjiang Formations (T_1j) and in Section 2 of the Leikoupo Formation (T_2l) and served as seal rocks of the natural gas reservoir in the Changxing-Feixianguan formations of the Puguang gas field (Ma et al., 2007a, b, in Fig. 2).

2 DATA AND PALEO-THERMAL RECONSTRUCTION

2.1 Paleogeothermal Indicator Data

Vitrinite reflectance (*R*o) and AFT are the most commonly used indicators for paleotemperature reconstruction. *R*o is the most commonly used indicator for organic matter maturity and can reveal the maximum paleotemperature. Although the annealing kinetics of various apatite grains differ slightly from one another, the annealing threshold is set to ~60 °C, while the full annealing temperature ranges between 120 °C and ~150 °C (Armstrong, 2005; Ketcham, 2005; Ketcham et al., 1999;

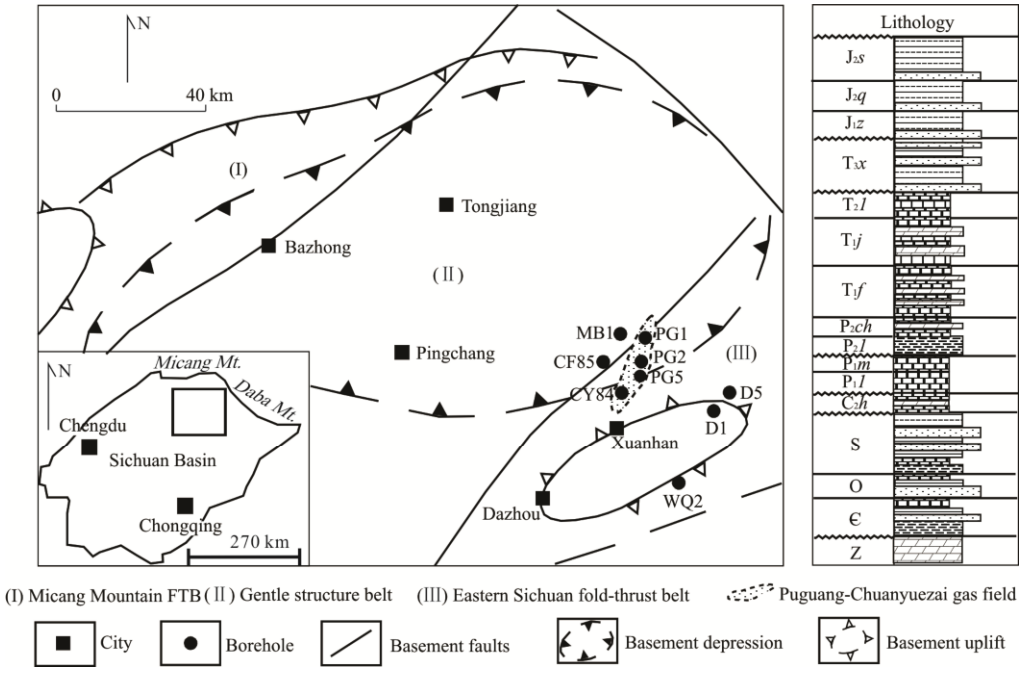

Figure 1. Distribution of boreholes, sketch of basement structures, and stratigraphic column of the northeastern Sichuan Basin (modified from Rao et al., 2011).

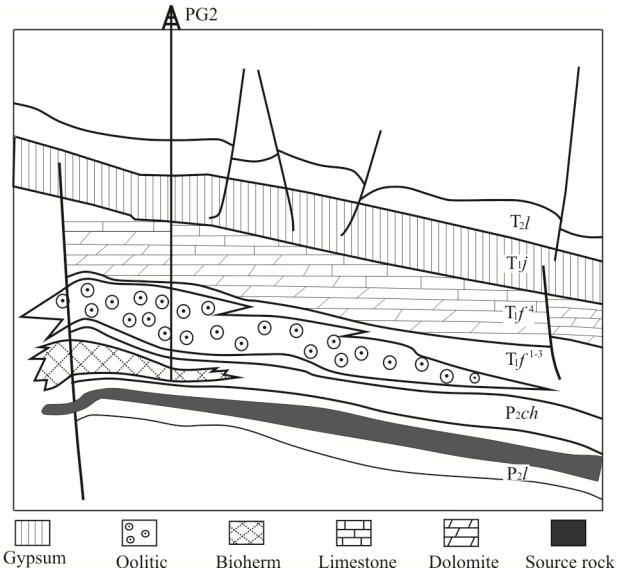

Figure 2. Cross-section of the Puguang 2 gas reservoir (modified from Ma et al., 2007a).

Green et al., 1986, 1985; Gleadow et al., 1983). Given this annealing behavior, AFT data can be used to reconstruct the thermal evolution of individual samples, especially the paleotemperature history in the AFT partial annealing temperature zone (PAZ) which ranges between ~60 and 125 °C (Gleadow et al., 1983).

The AFT data (Table 1 and Fig. 3) of Puguang boreholes were mainly sampled at depths greater than 3 500 m. The AFT age of a shallow sample from well PG2 (PG2-5, depth=370 m) is 70.2±5.1 (1σ) Ma and probably represents its depositional age. Remembering that depth increases with age, the fission track age of sample PG2-4 of 8.5±1.1 (1σ) Ma at ~3 500 m and the AFT ages of samples from well PG5 lie in the same range (Fig. 3), showing that the fission track ages of deeper samples are less than their deposition ages, indicating that the tracks of deeper samples have experienced annealing. The present geothermal gradient in this area (~20 °C/km) suggests that the present temperatures of samples PG2-5, PG2-6, and PG5-1 with mean track lengths of 12.10±1.8, 12.0±1.65 and 12.1±1.9 μm, respectively, are lower than the threshold temperature of ~60 °C at which apatite fission tracks commenced annealing. By contrast, the temperatures of samples PG5-8 and PG5-9 with mean track lengths of 10.3±2.2 and 11.2±2.0 μm, respectively, were in the range of the partial annealing zone of the current AFT.

*R*o values in PG 2 and PG5 are between 1.3% and 2.5%, and Jurassic *R*o values are between 1.3% and 2.0%, which indicates that the Jurassic *R*o is in a high maturity stage. Triassic *R*o values are all >2.0%, which suggests that the Triassic *R*o is in a post-maturity stage. Furthermore, at a depth of ~2 500 to 3 500 m, the *R*o values and increasing thermal gradients of PG2 and PG5 become consistent (Fig. 3).

2.2 Paleogeothermal Reconstruction Methods

Thermal history can be reconstructed using paleogeothermal indicators, such as low-temperature thermochronologic data such as AFT and (U-Th)/He, and organic matter maturity indicators (*R*o), by employing stochastic inversion (Gallagher, 1995; Corrigan, 1991; Lutz and Omar, 1991), paleotemperature gradient-based inversion (Hu et al., 2007; O'Sullivan, 1999; Bray et al., 1992; Duddy et al., 1988), and paleo-heat flow-based inversion (Lerche et al., 1984). We employed a stochastic inversion for the AFT data and the paleotemperature

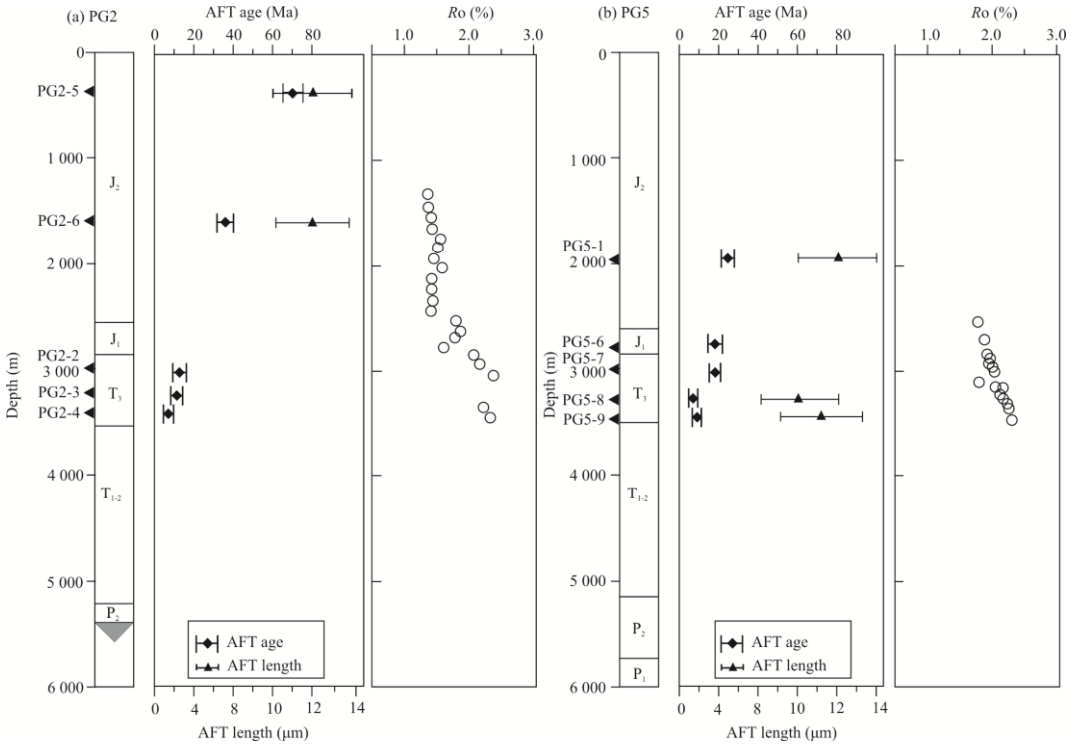

Figure 3. AFT and *R*o data of the samples of the Puguang boreholes.

Table 1 Apatite fission track data from boreholes PG2 and PG5*

No.	Depth (m)	Strata	NG	ρ_s (10^5/cm^2) (*N*s)	ρ_i (10^5/cm^2) (*N*i)	ρ_d (10^5/cm^2) (*N*d)	P (χ^2) (%)	Central age±1σ (Ma)	*L* (μm) (*N*L)
PG2-2	3 025.9	T_3x	20	1.758 (50)	44.29 (1 260)	16.48 (3 125)	99.9	12.7±1.9	
PG2-3	3 247.1	T_3x	21	0.667 (65)	17.54 (1 710)	15.39 (3 041)	96.2	11.4±1.5	
PG2-4	3 415.5	T_3x	20	0.761 (44)	32.78 (1 895)	14.80 (2 988)	77.7	6.7±1.0	
PG2-5	370.0	J_3p	21	4.82 (257)	19.82 (1 057)	14.92 (2 988)	83.8	70.2±5.1	12.10±1.8 (104)
PG2-6	1 590.0	J_2x	22	4.903 (182)	38.69 (1 436)	15.04 (2 988)	99.7	37.0±3.0	12.0±1.65 (106)
PG5-1	1 972.0	J_2q	19	2.435 (192)	3.932 (310)	2.113 (3 144)	79.0	24±3	l2.1±1.9 (19)
PG5-6	2 792.0	J_1z	21	1.713 (199)	4.131 (480)	2.113 (3 144)	11.3	17±2	
PG5-7	3 013.5	T_3x	10	2.422 (100)	5.062 (209)	2.029 (3 144)	24.5	17±3	
PG5-8	3 350.0	T_3x	28	0.640 (138)	3.880 (836)	2.134 (3 144)	4.4	7.0±0.8	10.3±2.2 (30)
PG5-9	3 508.0	T_3x	27	0.733 (191)	3.189 (831)	2.008 (3 144)	2.7	9.4±1.0	11.2±2.0 (16)

*Notes: No.. sample number, *N*. number of dated grains, *N*s. number of counted spontaneous tracks; *N*i. number of counted induced tracks; ρ_s. density of spontaneous tracks; ρ_i. density of induced tracks; *N*d. number of tracks on standard glass(CN-5); ρ_d. density of tracks on standard glass (CN-5); *L*. mean track length; *N*L. number of measured track lengths. The ages of PG2 samples were analyzed in the University of Melbourne (Tian et al., 2011) and calculated using a zeta value of 389.3±5.0 for CN5 with 12.2 ppm, while the ages of PG5 samples which were analyzed in China University of Geosciences, Beijing used a zeta value of 385.0±12.0.

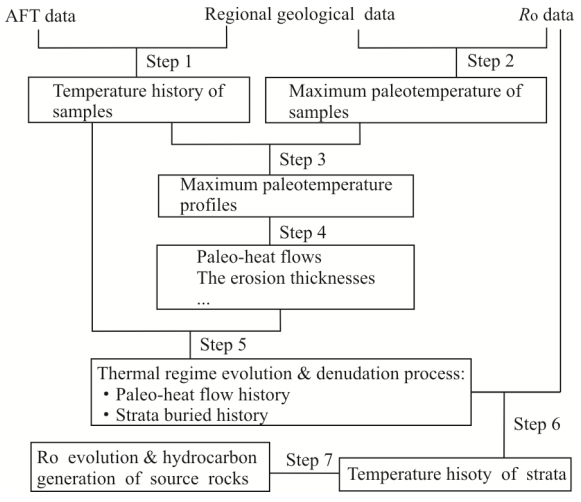

Figure 4. Flowchart of the thermal history modeling process based on AFT and *R*o data.

gradient-based inversion for the *R*o data to reconstruct the paleogeothermal history and determine the denudation thickness. We then modeled the thermal evolution and hydrocarbon generation history of the source rocks using these inverse results and other geologic parameters, such as the geochemistry of the source rocks and the thermal properties of the strata (Fig. 4).

The principles and modeling of low-temperature thermochronologic methods have been widely introduced and continuously developed (Ketcham et al., 2007; Armstrong, 2005; Fitzgerald et al., 1993; Fitzgerald and Gleadow, 1990; Gleadow and Fitzgerald, 1987; Gleadow et al., 1983; Gleadow, 1981; Naeser, 1979). The thermal histories of the samples have been reconstructed via a stochastic inversion method (Corrigan, 1991) and a Monte Carlo method based on an AFT annealing model (Ketcham et al., 2007) using the HeFty v1.7.4 software (Fig. 4, Step 1).

Many scholars have studied the model dynamics of vitrinite reflectance evolution to obtain the activation energy distributions of different types of kerogen (Sweeney and Burnham, 1990; Burnham and Sweeney, 1989; Burnham et al., 1989, 1987; Larter, 1989; Braun and Burnham, 1987; David and Antia, 1986; Tissot and Espitalie, 1975). The EASY *R*o% model (Sweeney and Burnham, 1990) is currently the most widely applied method for inverting the maximum paleotemperatures using *R*o data, because of its maturity and conciseness (Fig. 4, Step 2).

The model proposes that a series of successive sedimen-

tary strata reach their maximum temperatures simultaneously under steady-state heat conduction conditions. Therefore, a paleogeothermal gradient upon reaching the maximum paleotemperature can be obtained, based on the maximum temperatures of a series of samples (*R*o or AFT) at different depths (Fig. 4, Step 3). The paleo-heat flow and erosion thickness can be determined similarly (Fig. 3, Step 4).

In contrast to the paleotemperature gradient-based method, AFT modeling can directly estimate the time at which a sedimentary section began to cool down from its maximum paleotemperature. Therefore, combining *R*o with AFT provides a consistent integrated interpretation of the reconstructed thermal history of the boreholes, the paleogeothermal regime evolution (maximum paleotemperature gradient and heat flow), and the denudation process (uplift period and erosion thickness) (Fig. 4, Step 5).

Combining the burial and denudation information from the samples' thermal history obtained from AFT and considering the current heat flow as a constraint, the heat flow history of a borehole can be reconstructed using the paleo-heat flow method (Lerche, 1990; Lerche et al., 1984). The geothermal history of the strata is then reconstructed from the heat flow and strata burial histories (Fig. 4, Step 6). Based on the *R*o evolution dynamic model (i.e., the EASY% *R*o model), the maturity evolution and hydrocarbon generation history of the source rocks can be modeled (Fig. 4, Step 7).

2.3 Paleogeothermal Evolution and Denudation in Puguang Area and Thermal Evolution of Source Rocks

2.3.1 Thermal history and erosion thickness

Figure 5 shows the thermal history modeling results for samples from PG2 and PG5 computed from AFT data. The results for the PG2-5, PG2-6, and PG5-1 samples indicate that after the burial of these samples and allowing for possible slight cooling between 140 to 130 Ma, the entire process was continuous burial up to 90±10 Ma. After reaching the maximum paleotemperature at 90 Ma, cooling commenced and continued, indicating that uplift and denudation of northeastern Sichuan has continued since the Late Cretaceous era. Samples PG2-6 and PG5-1 and the other deeper samples cannot be used to reveal their exact maximum paleotemperatures upon entering the full annealing zone, although approximate maximum paleotemperatures can be estimated because these samples are located within the AFT full annealing zone. The samples experienced their maximum paleotemperatures at ~90 Ma. The maximum temperature of PG2-5 is ~90 °C, lower than the full annealing AFT temperature and indicated by excellent traces. On the basis of the combined results a relatively accurate burial and denudation history can be revealed. The strata reached their maximum paleotemperatures, indicating maximum burial depth under normal thermal evolution, in the Late Cretaceous era and were then uplifted and cooled continuously until the present.

The denudation processes can also be revealed by the cooling history, but the thickness of eroded strata cannot be accurately determined from low temperature thermal chronology modeling because the paleotemperature gradient cannot be constrained by a single sample. Assuming that the cooling resulted from denudation and occurred under a constant paleothermal gradient of ~20 °C/km similar to that of the present day, Tian et al. (2011) estimated the total post-Early Cretaceous denudation of the northeastern Sichuan Basin as ~5 km. Lu et al. (2005) considered the maximum erosion in the northeastern Sichuan Basin indicated by the Mesozoic–Cenozoic unconformity and obtained a mean value of ~2 100 m. However, our paleo-heat flow-based modeling results show that the erosion thickness of PG2 is 2 750 m, thereby indicating a huge difference between the results from low temperature thermal chronology modeling and paleo-heat flow-based modeling. Given that these two studies and other previous works have not obtained paleogeothermal gradient results, the accuracy of erosion thickness could not be evaluated.

The maximum gradients (*G*m) shown as dashed and dotted lines in Fig. 6 are calculated using the maximum paleotemperatures reconstructed from *R*o and AFT data, and the present temperature gradients (*G*p) are calculated measurements in the Puguang area (Xu et al., 2011; Lu et al., 2005). The erosion thickness (*E*) above PG2 has been computed as *E*(PG2)=[Tm(PG2)–10 °C (paleo-surface temperature)]/*G*m(PG2)= ~2.5 km. The erosion thickness of PG5 is computed as *E*(PG5)= [Tm(PG5)–10 °C (paleo-surface temperature)]/*G*m(PG5)= ~2.9 km. Heat flow (*q*) values are calculated from the temperature gradients (*G*) and thermal conductivity (*k*) of the strata as $q = G \times k$. The present thermal conductivity (*k*) of the boreholes are the harmonic mean values (~2.31 W/(m·K)) calculated from measured values (Lu et al., 2005) of the rocks and the component proportions different lithology in the lithological column of the boreholes because paleothermal conductivity can be inverted from its present value, and paleo-porosity and paleo-heat flow can be determined accordingly. Paleotemperatures are reconstructed using Thermodeo for Windows 2008.

The inversion results for *R*o and AFT data obtained by the paleogeothermal gradient method described in Fig. 6 reveal that the paleogeothermal gradient before denudation was approximately 30.0 °C/km and that the erosion thickness since the Late Cretaceous era was approximately 2.7±0.2 km (mean erosion thicknesses of PG2 and PG5). The paleogeothermal gradient was higher than the current values in the same geological setting (~20 °C/km) thereby reflecting cooling and uplift processes in the Puguang area since the Late Cretaceous era (~90 Ma).

2.3.2 Thermal evolution of the source rocks

Figure 7 shows the reconstructed maturity history of the source rocks of PG2. As a result of the Caledonian movement-driven uplift from Late Silurian to Early Carboniferous eras, the Lower Silurian source rocks only reached the hydrocarbon generation threshold in the Late Carboniferous era. During the high heat flow period in the Late Permian era (~260 Ma) (Zhu et al., 2016, 2010a; Rao et al., 2013), the Lower Silurian source rocks evolved further and entered the oil generation peak. The Jurassic era was the most important hydrocarbon generation period for the Permian and Silurian source rocks, and the thermal evolution process entered a post-maturity state (dry gas phase) after experiencing an oil generation peak in the Triassic era. According to Ma et al. (2007a), the Silurian and

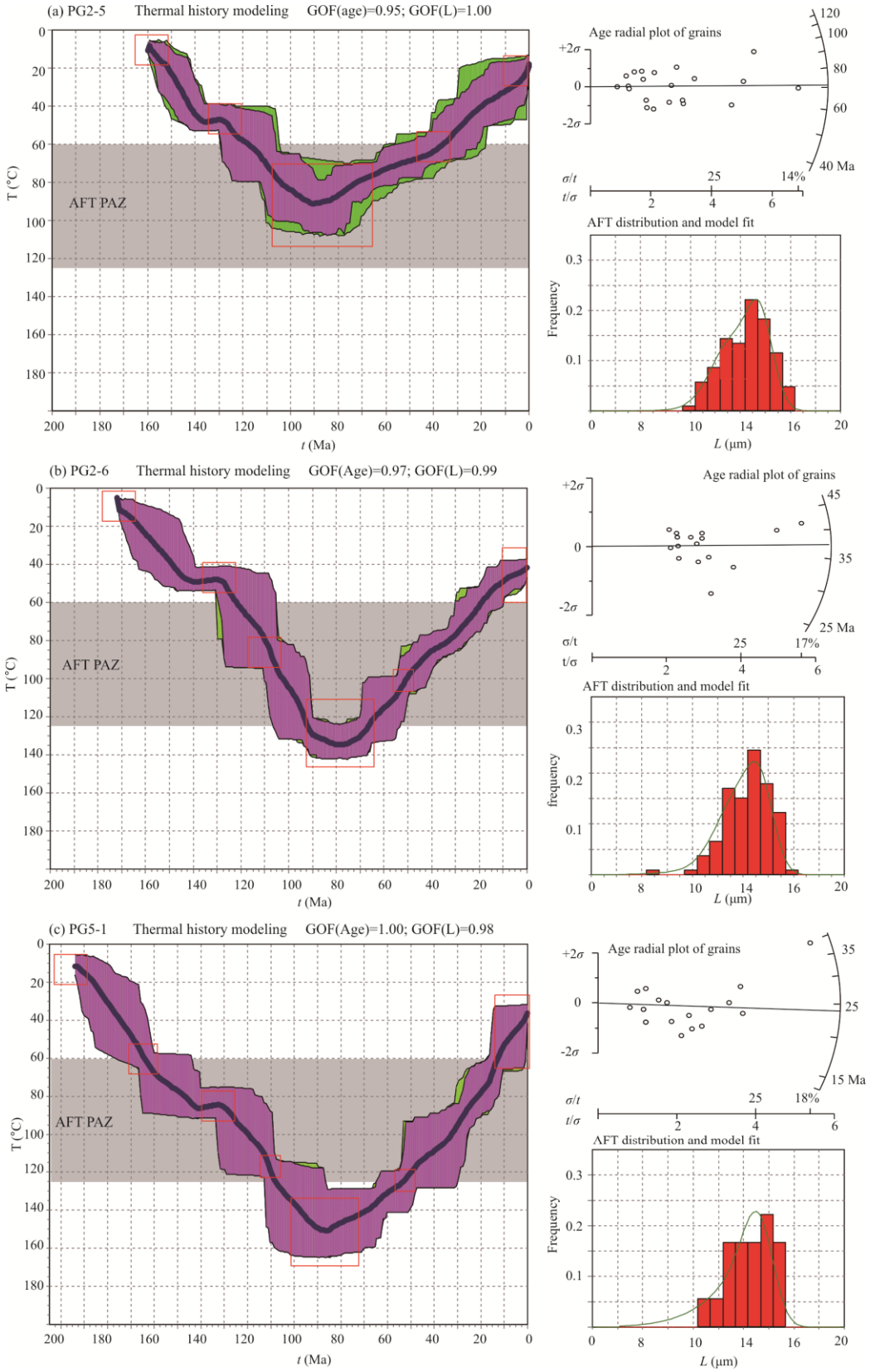

Figure 5. Thermal history modeling results of the AFT samples. A total of 10 000 paths have been modeled using the Monte Carlo method. Red rectangles indicate sample age and temperature ranges, and incorporate other regional geological data. The inversion results are a series of possible or equivalent thermal history paths that constitute a probability-distribution band. The width and dispersion of the band depend on the complexity of its thermal history, where a more complex thermal history exhibits a wider distribution band and greater uncertainty. Green regions indicate the envelopes of "acceptable traces" (0.4≤GOF<0.6), and purple regions indicate the envelopes of "good traces" (0.6≤GOF≤1.0). The bold blue line in each result indicates the mean of "good traces." The goodness of fit (GOF) of these results is indicated in bar charts to the lower right of each result, where green curves indicate the fit of the AFT length distribution above.

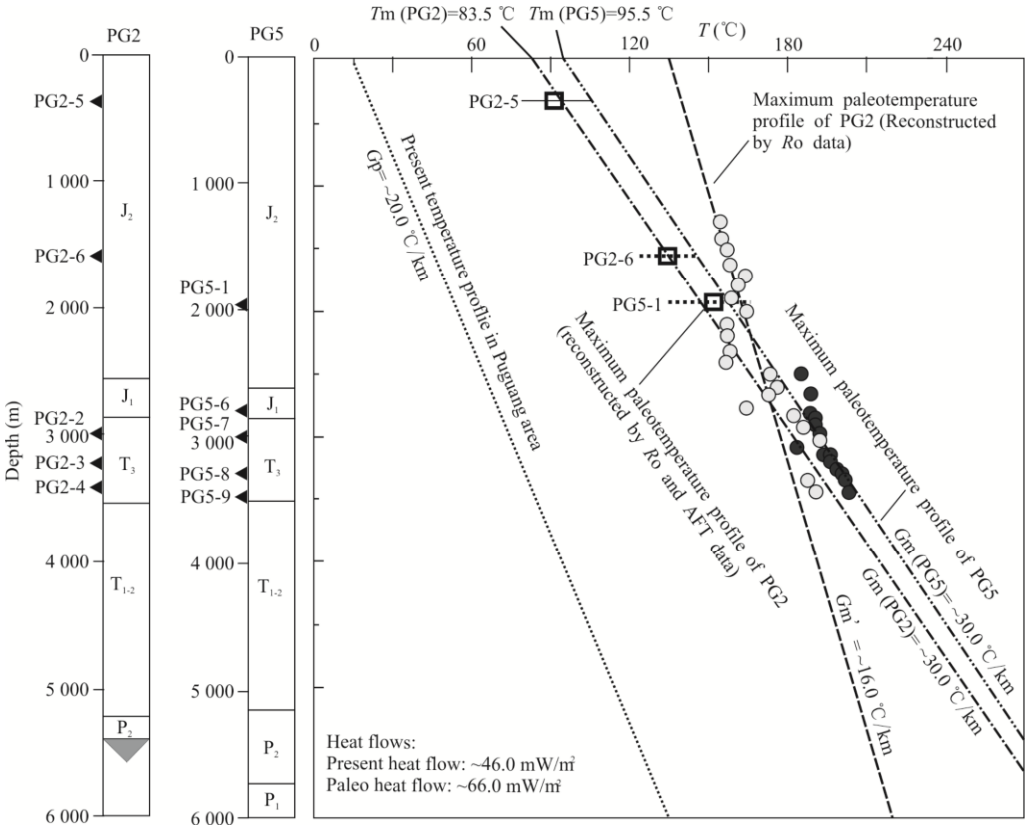

Figure 6. Maximum paleotemperature profiles reconstructed for PG2 and PG5. The result of PG2 which constrained by both *R*o and AFT data are more reliable than the profile which reconstructed based only on *R*o data.

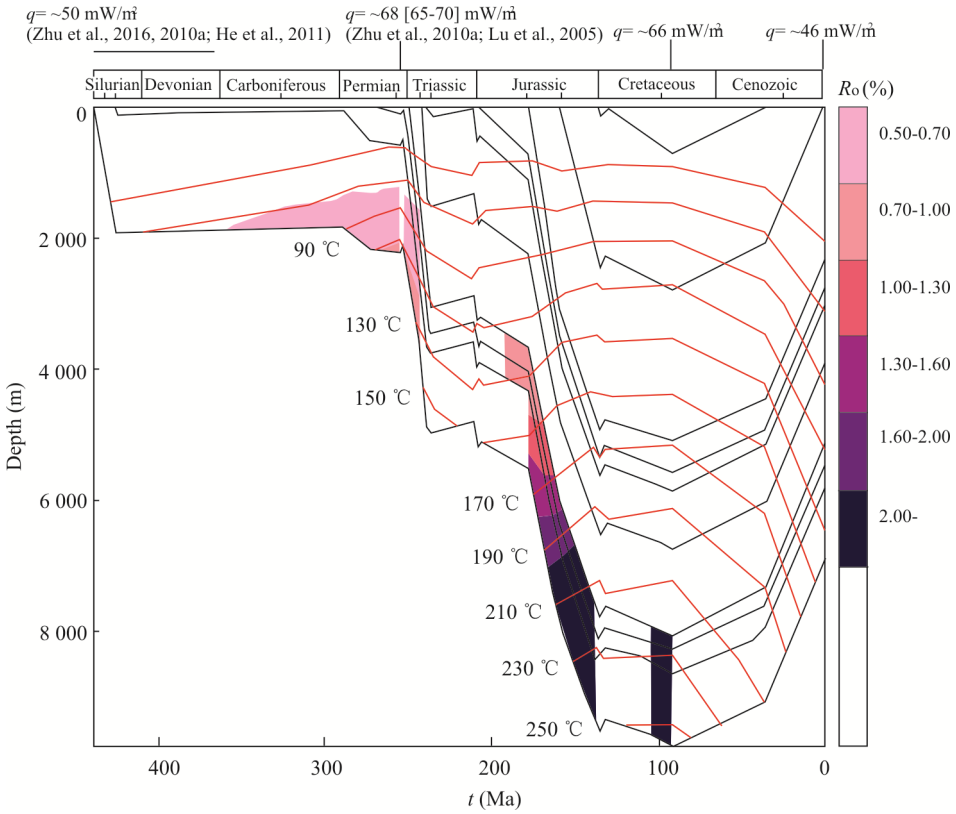

Figure 7. Burial depths (black lines) and isotherms (labeled red lines) of source rocks of well Puguang 2. The paleo-heat flows in the Late Cretaceous era and the present have been imported as determinate restraints for heat flow history. Previous works on the paleo-heat flow in the northeastern Sichuan Basin (Zhu et al., 2016, 2010a; He et al., 2011; Lu et al., 2005) were considered in arriving at the complete evolution.

Permian source rocks reached a hydrocarbon generation threshold in the Early Triassic era, the oil generation peak occurred in the Early Mid-Jurassic era, and the post-maturity evolution state occurred either in the late Mid-Jurassic era or the Late Jurassic era. Wu and Peng (2013) argued that the Permian source rocks generated hydrocarbon rapidly during the Late Triassic and Mid-Jurassic eras. Other studies identified the Jurassic era as one of the main hydrocarbon generation periods for the Silurian and Permian source rocks in this region. Given these conflicting versions of the heat flow history and denudation process, our proposed time windows for when the source rocks entered the oil threshold and when the hydrocarbon generation was terminated differ from those previously proposed although our proposed main hydrocarbon generation periods are somewhat in agreement with those of previous research.

3 THERMAL EVOLUTION CONDITIONS FOR NATURAL GAS ACCUMULATION

3.1 Hydrocarbon Generation and Accumulation Period

Petroleum accumulation depends on the configuration of hydrocarbon generation as well as migration, Formation, and evolution of the reservoir and its sealing conditions. The Silurian and Permian source rocks reached their oil and gas generation peaks in the Late Triassic era and in the Jurassic era respectively (Fig. 8), both later than the formation of the reservoir and seal rocks. The hydrocarbon generation period provided favorable conditions for the accumulation of oil and gas from these Silurian and Permian source rocks. Given the multiple phases of hydrocarbon generation, the Paleozoic source rocks in the northeastern Sichuan Basin had more favorable conditions for hydrocarbon accumulation than those in the southwest and other regions (Zhu et al., 2010b).

Evaporites and deeply buried, highly evolved mudstones are the most important oil and gas cap rocks (Zhou et al., 2013). In the Puguang structure well-developed gypsoliths are observed in sections 2 and 4 of the Lower Triassic Jialingjiang Formation and in Section 2 of the Middle Triassic Leikoupo Formation (Fig. 2), thereby constituting high-quality regional seal strata for the Changxing-Feixianguan formations gas reservoirs. These gypsoliths possessed great plasticity and maintained lateral continuity under the influence of tectonic stress, giving them a remarkable sealing capability (Ma et al., 2007a) to protect the petroleum reservoirs from uplift and deformation since the Late Cretaceous era. In this case, hydrocarbon generation from source rocks has a well-configured relationship with reservoir-seal evolution for petroleum accumulation. In addition, crude oil cracking gas in the Lower Triassic reservoir resulting from the formation of gypsolith seal rocks (Lu et al., 2005) reached its production peak during the Cretaceous era. All these conditions were favorable for the preservation of cracking gas.

3.2 Thermal Regime Changes during Hydrocarbon Generation and Preservation

The end of the Cretaceous era saw uplift and denudation in the Puguang area as well as a reduced geothermal gradient to cause complex processes of uplift, denudation, and basin cooling (Figs. 5 and 6). Consequently in the Triassic, strata temperatures decreased between 80 and 120 °C (Fig. 7). The relatively low temperature and geothermal gradient in this area with an average value of ~20 °C/km (Xu et al., 2011; Lu et al., 2005) favored the preservation of gas reservoirs and ensured the survival of hydrocarbons in deep strata. In terms of geothermics, either the configuration of the hydrocarbon generation timing in source rocks and reservoir cap development or the low geothermal field background after the formation of cracked gas provided favorable conditions for hydrocarbon accumulation in the northeastern Sichuan Basin.

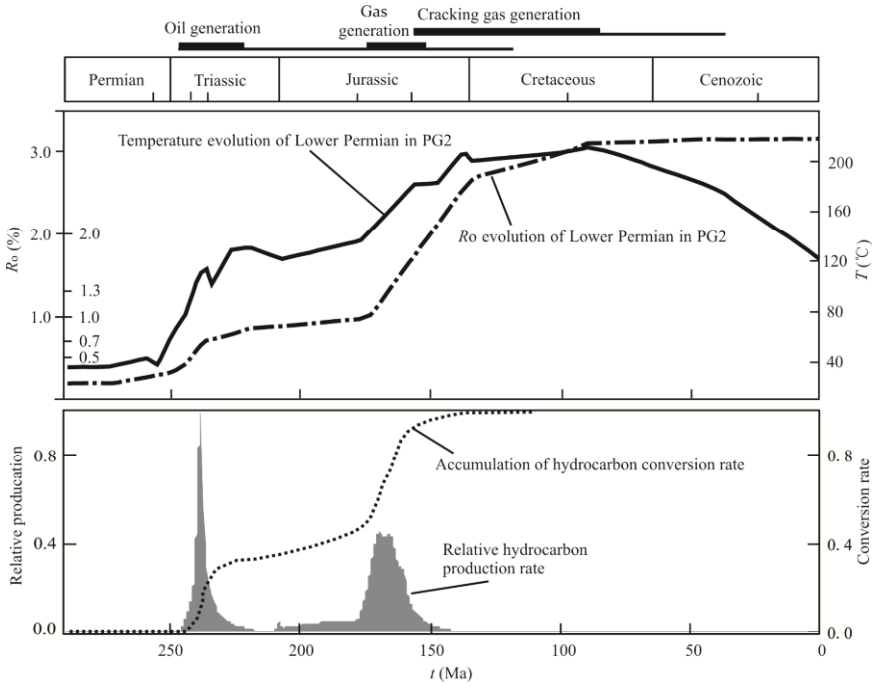

Figure 8. Thermal evolution and hydrocarbon generation history of the Permian source rock of PG2.

The Silurian and Permian shale gas and source rock gas resources in this region have also attracted attention over recent years (Gong et al., 2014; Liu et al., 2013; Huang, 2012). Temperature evolution affected the development of organic matter pores in strata and their gas adsorption capacity. In sum, a higher temperature and a greater extent of thermal evolution should have resulted in highly developed organic matter pores (Schieber, 2011; Loucks et al., 2009; Jarvie et al., 2007), whereas a lower temperature should have enhanced the gas adsorption capacity (Feng et al., 2012; Ross and Bustin, 2007). As shown in Fig. 7, the high temperature of the Permian source rocks, which may be attributed to the high temperature gradient and deep burying level of these rocks before their denudation in the Late Cretaceous era, was highly favorable for the maturity of organic matter and the development of their pores, whereas the cooling process after the main hydrocarbon and oil cracking gas generation periods benefited the preservation of source rock gas (shale gas).

4 CONCLUSIONS

(1) AFT modeling results indicate that except for slight cooling at approximately 140 to 130 Ma, the Puguang area has experienced continuous burial and warming from the Jurassic era to 90±10 Ma. After this maximum paleotemperature at ~90 Ma, cooling commenced and continued, indicating lasting uplift and denudation of northeastern Sichuan since the Late Cretaceous era.

(2) Maximum paleotemperature reconstruction indicates that when the strata reached their maximum temperature, the geothermal gradient was approximately 30 °C/km and the erosion thickness approximately 2.7±0.2 km. The paleogeothermal gradient and paleo-heat flow were higher than their current values, indicating continuous uplift and cooling in the basin since the Late Cretaceous era.

(3) The Jurassic era was the most significant hydrocarbon generation period for Silurian and Permian source rocks during which the thermal evolution entered into a post-maturity phase (dry gas stage) instead of the oil generating peak in the Triassic era. The thermal evolution process (warming and hydrocarbon generation followed by cooling after the formation of a reservoir cap system) of the source rocks in the northeastern Sichuan Basin provided the necessary geothermal conditions for the accumulation of conventional oil-gas and of unconventional hydrocarbons such as shale gas.

ACKNOWLEDGMENTS

This study was supported by the National Key Basic Research Development Plan of China (No. 2012CB214703), the National Natural Science Foundation of China (No. 41102152), the PetroChina Innovation Foundation (No. 2013D-5006-0102) and the Science Foundation of China University of Petroleum, Beijing (No. YJRC2013- 002). We would like to acknowledge comments from two anonymous reviewers and the suggestions provided by the editors. The final publication is available at Springer via http://dx.doi.org/10.1007/s12583-016-0909-8

REFERENCES CITED

Armstrong, P. A., 2005. Thermochronometers in Sedimentary Basins. *Reviews in Mineralogy and Geochemistry*, 58(1): 499–525

Braun, R. L., Burnham, A. K., 1987. Analysis of Chemical Reaction Kinetics Using A Distribution of Activation Energies and Simpler Models. *Energy & Fuels*, 1(2): 153–161

Bray, R. J., Green, P. F., Duddy, I. R., 1992. Thermal History Reconstruction Using Apatite Fission Track Analysis and Vitrinite Reflectance: A Case Study from the UK East Midlands and Southern North Sea. *Geological Society*, *London*, *Special Publications*, 67(1): 3–25

Burnham, A. K., Braun, R. L., Gregg, H. R., et al., 1987. Comparison of Methods for Measureing Kerogen Pyrolysis Rates and Fitting Kinetic Parameters. *Energy & Fuels*, 1: 452–458

Burnham, A. K., Oh, M. S., Craford, R. W., 1989. Pyrolysis of Argonne Premium Coals: Activation Energy Distribution and Related Chemistry. *Energy & Fuels*, 3(1): 42–55

Burnham, A. K., Sweeney, J. J., 1989. A Chemical Kinetic Model of Vitrinite Maturation and Reflectance. *Geochimica et Cosmochimica Acta*, 53(10): 2649–2657

Cai, L. G., Rao, D., Pan, W. L., et al., 2005. The Evolution Model of the Puguang Gas Field in Northeast of Sichuan. *Petroleum Geology & Experiment*, 27(5): 462–467 (in Chinese with English Abstract)

Corrigan, J., 1991. Inversion of Apatite Fission Track Data for Thermal History Information. *Journal of Geophysical Research*, 96: 347–360

David, D., Antia, J., 1986. Kinetic Method for Modeling Vitrinite Reflectance. *Geology*, 14(7): 606–608

Duddy, I. R., Green, P. F., Lastett, G. M., 1988. Thermal Annealing of Fission Tracks in Apatite, 3. Aariable Temperature Behaviour. *Chemical Geology*, 73: 25–38

Feng, Y. Y., Chu, W., Sun, W. J., 2012. Adsorption Characteristics of Methane on Coal under Reservoir Temperatures. *Journal of China Coal Society*, 37(9): 1488–1492 (in Chinese with English Abstract)

Fitzgerald, P. G., Gleadow, A. J. W., 1990. New Approaches in Fission Track Geochronology as a Tectonic Tool: Examples from the Transantarctic Mountains. *International Journal of Radiation Applications and Instrumentation. Part D. Nuclear Tracks and Radiation Measurements*, 17(3): 351–357

Fitzgerald, P. G., Stump, E., Redfield, T. F., 1993. Late Cenozoic Uplift of Denali and Its Relation to Relative Plate Motion and Fault Morphology. *Science*, 259(5094): 497–499

Gallagher, K., 1995. Evolving Temperature Histories from Apatite Fission-Track Data. *Earth and Planetary Science Letters*, 136: 421–435

Gleadow, A. J. W., Duddy, I. R., Green, P. F. et al., 1983. Fission Track Analysis: A New Tool for the Evaluation of Thermal Histories and Hydrocarbon Potential. *Australian Petroleum Exploration Association Journal*, 23: 93–102

Gleadow, A. J. W., Fitzgerald, P. G., 1987. Uplift History and Structure of the Transantarctic Mountains: New Evidence from Fission Track Dating of Basement Apatites in the Dry Valleys Area Southern Victoria Land. *Earth and*

Planetary Science Letters, 82(1–2): 1–14

Gleadow, A. J. W., 1981. Fission-Track Dating Methods: What Are the Real Alternatives? *Nuclear Tracks*, 5(1–2): 3–14

Gong, L., Wang, C. Y., Yang, Y. G., et al., 2014. Comparion of Reservoir-Forming Conditions and Objective Exploration Zones of Shale Gas in Lower Silurian Longmaxi Formation of Southwest and Northeast Sichuan Basin. *Geological Science and Technology Information*, 33(5): 128–133 (in Chinese with English Abstract)

Green, P. F., Duddy, I. R., Gleadow, A. J. W., et al., 1985. Fission Track Annealing IN Apatite: Track Length Measurements and the Form of the Arrhenius Plot. *Nuclear Tracks*, 10: 323–328

Green, P. F., Duddy, I. R., Gleadow, A. J. W., et al., 1986. Thermal Annealing of Fission Tracks in Apatite, 1. A Qualitative Description. *Chemical Geology*, 59: 237–253

He, L. J., Xu, H. H., Wang, J. Y., 2011. Thermal Evolution and Dynamic Mechanism of the Sichuan Basin during the Early Permian–Middle Triassic. *Science China*: *Earth Sciences*, 54(12): 1948–1954

Hu, S. B., Fu, M. X., Yang, S. C., et al., 2007. Palaeogeothermal Response and Record of Late Mesozoic Lithospheric Thinning in the Eastern North China Craton. In: Zhai, M. G., Windley, B. F., Kusky, T. M., et al., eds., Mesozoic Sub-Continental Lithospheric Thinning under Eastern Asia. *Geological Society*, *London*, *Special Publications*, 280: 267–280

Huang, J. Z., Chen, S. J., Song, J. R., et al., 1996. Hydrocarbon Source Systems and Formation of Gas Fields in Sichuan Basin. *Science in China* (*Series D*), 40(1): 32–42 (in Chinese with English Abstract)

Huang, J. Z., 2012. Prospect of Source Rock Gas Based on Shale Gas Accumulation Patterns: A Cas Study from the Low Permian in the Sichuan Basin. *Natural Gas Industry*, 32(11): 4–9 (in Chinese with English Abstract)

Jarvie, D. M., Hill, R. J., Ruble, T. E., et al., 2007. Unconventional Shale-Gas Systems: The Mississippian Barnett Shale of North-Central Texas as One Model for Thermogenic Shale-Gas Assessment. *AAPG Bulletin*, 91(4): 475–499

Ketcham, R. A., Donelick, R. A., Carlson, W. D., 1999. Variabilityof Apatitefission Track Annealing Kinetics: III. Extrapolation to Geological Timescales. *American Mineralogist*, 84(9): 1235–1255

Ketcham, R. A., 2005. Forward and Inverse Modeling of Low Temperature Thermochronometry Data. *Reviews in Mineralogy and Geochemistry*, 58: 275–314

Ketcham, R. A., Carter, A., Donelick, R. A., et al., 2007. Improved Modeling of Fission-Track Annealing in Apatite. *American Mineralogist*, 92: 799–810

Larter, S., 1989. Chemical Models of Vitrinite Reflectance Evolution. *Geologische Rundschau*, 78(1): 349–359

Lerche, I., Yarzab, R. F., Kendall, C. G., 1984. Determination of Paleoheat Flux from Vitrinite Reflectance Data. *AAPG Bulletin*, 68(11): 1704–1717

Lerche, I., 1990. Basin Analysis: Quantitative Methods Volume I. Academic Press Inc., San Diego. 74–96

Liang, D. G., Guo, T. L., Chen, J. P., et al., 2008. Distribution of Four Suits of Regional Marine Source Rocks. *Marine Origin Petroleum Geology*, 13(2): 1–16 (in Chinese)

Liu, D. H., Xiao, X. M., Tian, H., et al., 2013. Multiple Types of High Density Methane Inclusions and their Relationships with Exploration and Assessment of Oil-Cracked Gas and Shale Gas Discovered in NE Sichuan. *Earth Science Frontiers*, 20(1): 64–71 (in Chinese with English Abstract)

Loucks, R. G., Reed, R. M., Ruppel, S. C., et al., 2009. Morphology, Genesis, and Distribution of Nanometer-Scale Pores in Siliceous Mudstones of the Mississippian Barnett Shale. *Journal of Sedimentary Research*, 79(12): 848–861

Lu, Q. Z., Hu, S. B., Guo, T. L., et al., 2005. The Background of the Geothermal Field for Formation of Abnormal High Pressure in the Northeastern Sichuan Basin. *Chinese Journal of Geophysics*, 48: 1110–1116 (in Chinese with English Abstract)

Lutz, T. M., Omar, G., 1991. Inverse Methods of Modeling Thermal Histories from Apatite Fission Track Data. *Earth and Planetary Science Letters*, 104: 181–195

Ma, Y. S., Cai, X. Y., Guo, T. L., et al., 2007a. The Controlling Factors of Oil and Gas Charging and Accumulation of Puguang Gas Field in the Sichuan Basin. *Chinese Science Bulletin*, 52 (Suppl. I): 193–200 (in Chinese with English Abstract)

Ma, Y. S., Guo, X. S., Guo, T. L., et al., 2007b. The Puguang Gas Field: New Giant Discovery in the Mature Sichuan Basin, Southwest China. *AAPG Bulletin*, 91: 627–643

Ma, Y. S., 2010. Formation Mechanism of Deep-Buried Carbonate Reservoir and Its Model of Three-Element Controlling Reservoir: A Case Study from the Puguang Oil Field in Sichuan. *Acta Geologica Sinica*, 84(8): 1087–1094 (in Chinese with English Abstract)

Mei, L. F., Liu, Z. Q., Tang, J. G., et al., 2010. Mesozoic Intra-Continental Progressive Deformation in Western Hunan-Hubei Eastern Sichuan Provinces of China: Evidence from Apatite Fission Track and Balanced Cross-Section. *Earth Science—Journal of China University of Geosciences*, 35(2): 161–174 (in Chinese with English Abstract)

Naeser, C. W., 1979. Thermal History of Sedimentary Basins: Fission Track Dating of Subsurface Rocks. In: Scholle, P. A. Schluger, P. R., eds., Aspects of Diagenesis. *Society of Economic Paleotologists and Mineralogists Special Publication*, 26: 109–112

O'Sullivan, P. B., 1999. Thermochronology, Denudation and Variations in Palaeosurface Temperature: A Case Study from the North Slope Foreland Basin, Alaska. *Basin Research*, 11: 191–204

Rao, S., Tang, X. Y., Zhu, C. Q., et al., 2011. The Application of Sensitivity Analysis in the Source Rock Maturity History Simulation: An Example from Palaozioc Marine Source Rock of Puguang-5 Well in the Northeast of Sichuan Basin. *Chinese Journal of Geology*, 46(1): 213–225 (in Chinese with English Abstract)

Qiu, N. S., Qin, J. Z., Brent, I. A. M., 2008. Tectonothermal Evolution of the Northeastern Sichuan Basin: Constraints

from Apatite and Zircon (U-Th)/He Ages and Vitrinite Reflectance Data. *Geological Journal of Chinese Universities*, 14: 223–230 (in Chinese with English Abstract)

Rao, S., Zhu, C. Q., Wang, Q., et al., 2013. Thermal Evolution Patterns of the Sinian-Lower Paleozoic Source Rocks in the Sichuan Basin, Sourthwest China. *Chinese Journal of Geophysics*, 56(5): 1549–1559 (in Chinese with English Abstract)

Ross, D. J. K., Bustin, R. M., 2007. Shale Gas Potential of the Lower Jurassic Gordondale Member, Northeastern British Columbia, Canada. *Bulletin of Canadian Petroleum Geology*, 55(1): 51–75

Schieber, J., 2011. Shale Microfabrics and Pore Development: An Overview with Emphasis on the Importance of Depositional Processes: Canadian Society of Petroleum Geologists, Canadian Society of Exploration Geophysicists, and Canadian Well Logging Society Joint Annual Convention. Calgary, Alberta. 4

Shen, C. B., Mei, L. F., Guo, T. L., 2007. Fission Track Analysis of Mesozoic–Cenozoic Thermal History in Northeast Sichuan Basin. *Natural Gas Industry*, 27: 24–26 (in Chinese with English Abstract)

Sweeney, J. J., Burnham, A. K., 1990. Evaluation of a Simple Model of Vitrinite Reflectance Based on Chemical Kinetics. *AAPG Bulletin*, 74: 1559–1570

Tenger, Liu, W. H., Qin, J. Z., et al., 2012. Dynamic Transformation Mechanism For Hydrocarbon Generation from Multiple Sources in Deep-Buried Marine Carbonates in the Northeastern Sichuan Basin: A Case Study from the Puguang Gas Field. *Acta Petrologica Sinica*, 28(3): 895–904 (in Chinese with English Abstract)

Tenger, Qin, J. Z., Fu, X. D., et al., 2010. Hydrocarbon Source Rocks Evaluation of the Upper Permian Wujiaping Formation in Northeast Sichuan Area. *Journal of Palaeogeography*, 12(3): 1–12 (in Chinese with English Abstract)

Tian, Y. T., Zhu, C. Q., Xu, M., et al., 2011. Post-Early Cretaceous Denudation History of the Northeastern Sichuan Basin: Constraints from Low-Temperature Thermochronology Profiles. *Chinese Journal Geophysics*, 54(3): 807–816 (in Chinese with English Abstract)

Tian, Y. T., Kohn, B. P., Zhu, C. Q., et al.,2012. Post-Orogenic Evolution of the Mesozoic Micang Shan Foreland Basin System, Central China. *Basin Research*, 24: 70–90

Tissot, B. P., Pelect, R. U., 1987. Thermal History of Sedimentary Basin Maturation Indices and Kinetics of Oil and Gas Generation. *AAPG Bulletin*, 71: 1445–1466

Tissot, B. P., Welte, D. H., 1984. Petroleum Formation and Occurrence. Springer Verlag, NewYork.

Tissot, B., Espitalie, J., 1975. L'Evolution Thernique de la Matiere Organique des Sediments: Applications Dune Simulation Mathematique. *Oil & Gas Science and Technology*, 30: 743–778

Wu, Q., Peng, J. N., 2013. Burial and Thermal Histories of Northeastern Sichuan Basin: A Case Study of Well Puguang 2. *Petroleum Geology & Experiment*, 35(2): 133–138 (in Chinese with English Abstract)

Xu, M., Zhu, C. Q., Tian, Y. T., et al., 2011. Well Temperature Logging and Characteristics of Subsurface Temperature in Sichuan Basin. *Chinese Journal of Geophysics*, 54: 1052–1060 (in Chinese with English Abstract)

Zhang, G. C., 2014. Analysis of the Regular Distribution of Oil and Gas Fields in China Based on the Theory of Hydrocarbon Generation Controlled by Source Rocks and Geothermal Heat. *Natural Gas Industry*, 34(5): 1–28 (in Chinese with English Abstract)

Zhang, G. C., 2012. Co-Control of Source and Heat: The Generation and Distribution of Hydrocarbons Controlled by Source Rocks and Heat. *Acta Petrolei Sinic*a, 33(5): 723–738 (in Chinese with English Abstract)

Zheng, R. C., Geng, W., Zheng, C., et al., 2008. Genesis of Dolostone Reservoir of Feixianguan Formation in Lower Triassic of Northeast Sichuan Basin. *Acta Petrolei Sinica*, 29(6): 815–821 (in Chinese with English Abstract)

Zhou, Y., Jin, Z. J., Zhu, D. Y., et al., 2013b. Current Status and Progress in Research of Hydrocarbon Cap Rocks. *Petroleum Geology & Experiment*, 34(3): 234–245 (in Chinese with English Abstract)

Zhu, C. Q., Xu, M., Yuan, Y. S., et al., 2010a. Paleogeothermal Response and Record of the Effusing of Emeishan Basalts in the Sichuan Basin. *Chinese Science Bulletin*, 55(10): 949–956

Zhu, C. Q., Tian, Y. T., Xu, M., et al., 2010b. The Effect of Emeishan Supper Mantle Plume to the Thermal Evolution of Source Rocks in the Sichuan Basin. *Chinese Journal of Geophysics*, 53(1): 119–127 (in Chinese with English Abstract)

Zhu, C. Q., Hu S. B., Qiu, N. S., et al., 2016. Thermal History of the Sichuan Basin, SW China: Evidence from Deep Boreholes. *Science China*: *Earth Sciences*, 59(1): 70–82